

Communication

Core/Shell Gel Beads with Embedded Halloysite Nanotubes for Controlled Drug Release

Lorenzo Lisuzzo ¹, Giuseppe Cavallaro ^{1,2}, Filippo Parisi ¹, Stefana Milioto ^{1,2},
Rawil Fakhruллин ³ and Giuseppe Lazzara ^{1,2,*}

¹ Dipartimento di Fisica e Chimica, Università degli Studi di Palermo, Viale delle Scienze, pad. 17, 90128 Palermo, Italy; lorenzo.lisuzzo@unipa.it (L.L.); giuseppe.cavallaro@unipa.it (G.C.); filippo.parisi@unipa.it (F.P.)

² Consorzio Interuniversitario Nazionale per la Scienza e Tecnologia dei Materiali, INSTM, Via G. Giusti 9, I-50121 Firenze, Italy; stefana.milioto@unipa.it

³ Institute of Fundamental Medicine and Biology, Kazan Federal University, Kremlyuramı 18, Kazan, Republic of Tatarstan 420008, Russia; kazanbio@gmail.com

* Correspondence: giuseppe.lazzara@unipa.it; Tel.: +39-091-2389-7962

Received: 15 November 2018; Accepted: 22 January 2019; Published: 24 January 2019



Abstract: The use of nanocomposites based on biopolymers and nanoparticles for controlled drug release is an attractive notion. We used halloysite nanotubes that were promising candidates for the loading and release of active molecules due to their hollow cavity. Gel beads based on chitosan with uniformly dispersed halloysite nanotubes were obtained by a dropping method. Alginate was used to generate a coating layer over the hybrid gel beads. This proposed procedure succeeded in controlling the morphology at the mesoscale and it had a relevant effect on the release profile of the model drug from the nanotube cavity.

Keywords: halloysite; alginate; chitosan; gel beads; drug release

1. Introduction

Researchers have defined hydrogels in many different ways, but nowadays the most accepted definition is the existence of a three-dimensional network, formed by the cross-linking of polymeric chains, that possesses the capability to swell thanks to the presence of hydrophilic groups and to maintain a very high amount of water in its structure [1,2]. Since their discovery, hydrogels have received attention from the scientific community due to the wide range of applications they can be used for: Environmental issues like water remediation, drug delivery systems and tissue engineering, cosmetic and food packaging industry, and oil spill recovery [3–8]. Furthermore, with the evolution of nanotechnology, the challenge to design and prepare hydrogels with specific and requested features at the nano-scale led to the development of nanohydrogels. Among the different polymeric species that can be used to achieve this aim, polysaccharides cover a marked importance, especially in the preparation of the so-called “polysaccharide-based natural hydrogels”, for some of their most peculiar properties such as water solubility and swelling capacity, biocompatibility and biodegradability, self-healing and pH sensitivity that are crucial for their use [9,10]. Moreover, the possibility to modify the structure of the polysaccharides and the adaptability of their networks allows for the development of eco-friendly smart materials [11,12]. To date, the most widely used raw materials include natural biopolymers such as chitosan, alginate, pectin and cellulose. One of the major factors limiting the use of nanohydrogels is their structural instability, thus making necessary the use, among others, of inorganic nanoparticles to overcome them [13–16].

Among clays, halloysite nanotubes (HNTs) have great importance thanks to their own main characteristics [17]. HNTs are a naturally occurring aluminosilicate whose structural formula is

$\text{Al}_2\text{Si}_2\text{O}_5(\text{OH})_4 \cdot n\text{H}_2\text{O}$, where Al is disposed in an gibbsite-like octahedral organization of Al–OH groups whereas Si–O groups form a tetrahedral sheet [18,19]. Both aluminols and siloxanes layers are overlapped in a kaolinite typical sheet that rolls up due to some structural defects and to the presence of water molecules, thus giving halloysite its peculiar narrow nanotubular structure [20–22].

HNTs dimensions depend on the natural deposit the clay is extracted from. In particular, the internal and external diameters are approximately 10–15 and 50–80 nm respectively, while the nanotubes length can range from 100 nm to 2 μm . [19] Interestingly, it is possible to classify halloysite by considering the distance between interlayers. For instance, it can be 7 or 10 Å depending on the number of water molecules present between the layers, which is namely 0 or 2, respectively [23,24]. Moreover, one of halloysite's most fascinating and important features is the different charge, in the pH interval from 3 to 8, between the outer surface that is mainly composed of Si–O groups and negatively charged, and the inner surface that is mainly composed of Al–OH and positively charged [25,26]. This different charge, due to the chemical composition, allows for selective functionalization, exploiting both the covalent and electrostatic interactions of each surface with other oppositely charged species: Drug molecules, polysaccharides, proteins, lipids, surfactants and so on [27–29]. All these features, and also considering that they are low cost, eco- and biocompatible materials [30], make HNTs suitable for designing hybrid materials for waste water remediation [31–35], cultural heritage treatment [36,37], biotechnological applications [38–44], and packaging [45–50].

Notably, halloysite is commonly used as a component in drug delivery systems through exploiting its characteristics in combination with other organic moieties, for example the temperature responsive polymers such as poly(N-isopropylacrylamide) (PNIPAAms) that can selectively interact with the inner/outer surfaces thus influencing the release kinetics by changing their adsorption site [51], or natural occurring biopolymers for the preparation of end capped nanotubes with smart gates, or reverse inorganic micelles for the formation of nanohydrogels inside the HNTs lumen for a triggered absorption or release [52,53].

As evidenced in a recent review [17], the combination of polymer hydrogels and hollow inorganic nanotubes represents a perspective strategy for the fabrication of functional carriers in an advanced application.

In this work, we prepared hydrogel beads based on chitosan containing halloysite nanotubes. An alginate layer was introduced by diffusion and immersion of the beads in a sodium alginate solution. The dispersion of nanotubes into the hybrid gel and the localization of the alginate was investigated by SEM and fluorescence microscopy. Doxycycline, an antibiotic of the tetracycline class, was used as the model drug and it was loaded into the halloysite cavity by using a literature protocol [54]. This work represents a promising step for a valid alternative to generate hybrid hydrogels with oppositely charged polysaccharides and nanoclay with specific morphology for controlled drug release.

2. Results and Discussion

2.1. Morphology of the Hybrid Gel Beads

Figure 1 shows the optical image of the prepared chitosan/HNTs gel beads covered with a calcium alginate layer. They had an average diameter of 3.5 mm that shrunk to 0.8 mm when dried. To highlight the halloysite nanotubes distribution in the beads, SEM images were taken and they showed the presence of halloysite nanotubes in a random orientation within the polymer matrix (Figure 1). Similar findings have been reported by us for alginate/halloysite gel beads [55]. The dispersibility of the nanoparticles could be explained by the affinity between the polymer and halloysite and the colloidal stability of the nanoclay in polymer solution [56]. It should be noted that the halloysite cavity did not interact with the chitosan polycation as the inner surface of the nanotubes was positively charged [26]. Therefore, the HNTs lumen was preserved for drug loading.

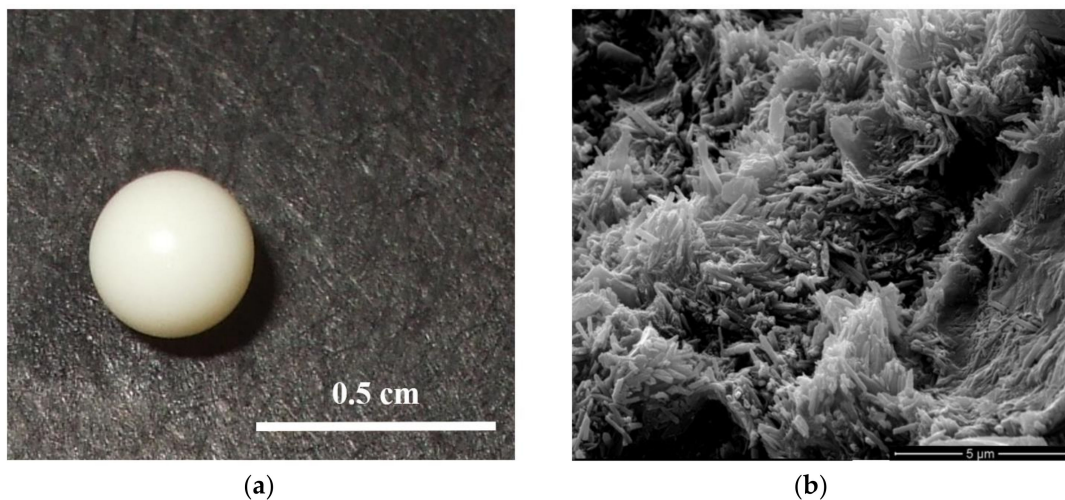


Figure 1. (a) Optical image of wet alginate/chitosan/halloysite nanotubes (HNTs) gel beads and (b) SEM image of the inner part of the dried gel beads.

Neither optical nor SEM imaging were able to identify the alginate location in the beads. We therefore thought to label the alginate polymer with a fluorescent probe 5-(4,6-dichlorotriazinyl) aminofluorescein (DTAF) that showed fluorescent emission when excited at 490 nm. Firstly, a blank experiment on chitosan/halloysite gel beads was carried out and negligible fluorescence was observed. The laser scanning confocal microscopy images on chitosan/HNTs gel beads covered with a calcium alginate layer clearly showed a fluorescent layer with an average thickness of approximately 130 μm , revealing that the diffusion of alginate into the chitosan/halloysite gel beads occurred up to a certain extent and the core of the beads was alginate free (Figure 2). On this basis, one could conclude that the simple preparation protocol allowed us to prepare a controlled complex architecture in mesoscopic scale that might be suitable for sustained release of active substances.

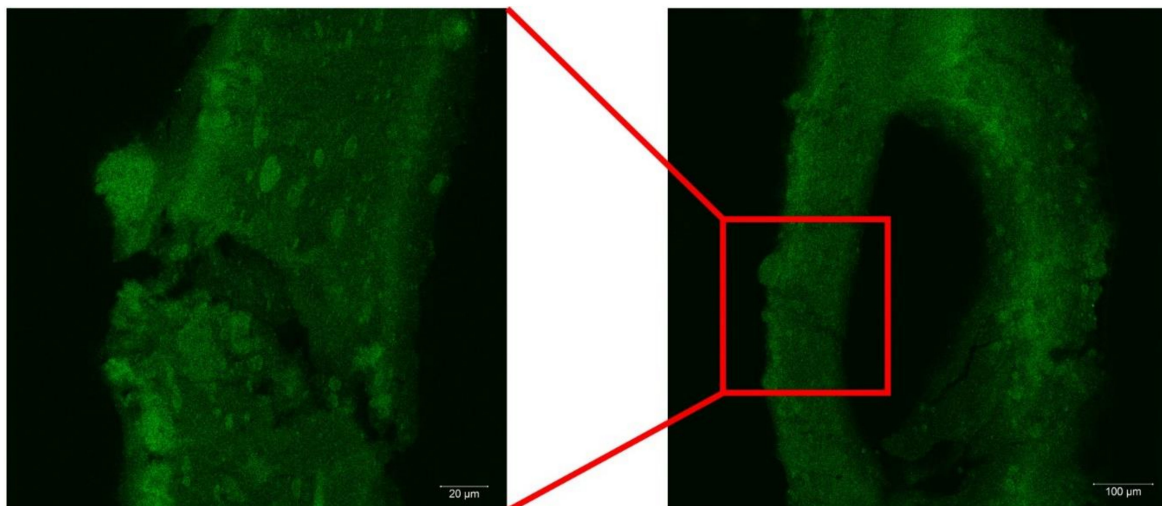


Figure 2. Laser scanning confocal microscopy images of alginate/chitosan/HNTs gel beads. Note that Alginate was labelled with 5-(4,6-dichlorotriazinyl) aminofluorescein (DTAF).

2.2. Drug Release Experiments

Release experiments were carried out by using doxycycline chlorohydrate as a model drug that could be loaded into the halloysite nanotubes [54]. The pK value for the drug was approximately 3 and the solubility dropped down as soon as the non-ionic form was obtained at $\text{pH} > \text{pK}$. Therefore, under our experimental conditions the drug was always neutral. The release profiles in water are

provided in Figure 3 for doxycycline from halloysite nanotubes, chitosan/HNTs dried beads and alginate/chitosan/HNTs dried beads. It was clearly observed that halloysite incorporation into chitosan gel beds only slightly slowed down the drug release from being fully available in the solvent media in 20 min. The sustained release was due to the slow release of the drug from the nanotube cavity and the subsequent drug diffusion through the polymer matrix to the solvent. The presence of an alginate coating significantly slowed down the doxycycline release from the hybrid beads. In particular after 20 min only 50% of the drug was released into the solvent media while a full release occurs in more than 80 min. These results could be interpreted by considering that the alginate shell in combination with the oppositely charged chitosan could generate a highly viscous layer that further delayed the drug diffusion from the beads to the solvent.

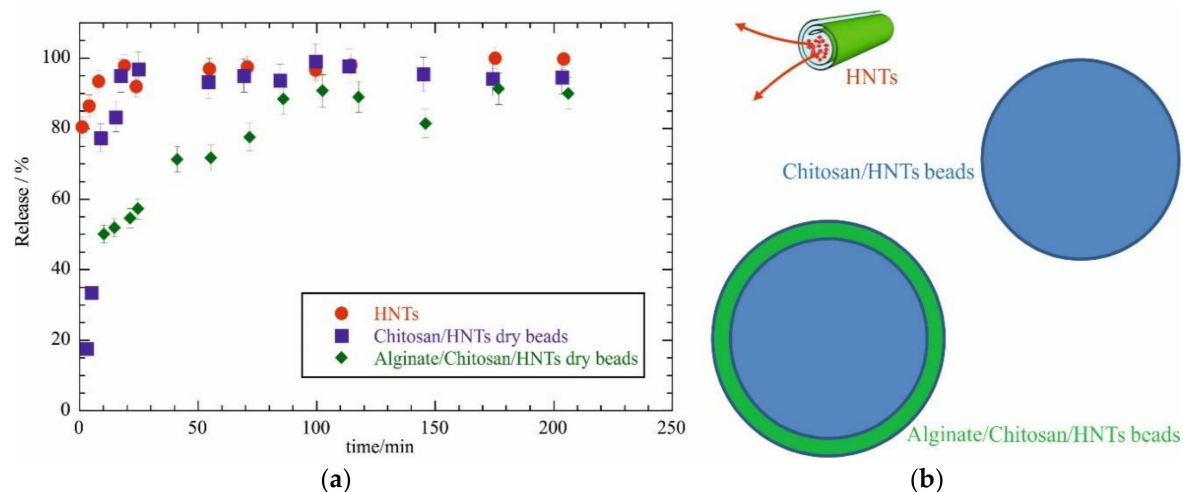


Figure 3. (a) Doxycycline chlorohydrate release as a function of time for different carriers. (b) Sketch view of the different release systems.

3. Materials and Methods

3.1. Materials

Halloysite, acetic acid, sodium hydroxide, ethylenediaminetetraacetic acid and DTAF, sodium alginate ($M_w = 70\text{--}100 \text{ kg mol}^{-1}$), and chitosan ($M_w = 50\text{--}190 \text{ kg mol}^{-1}$) were Sigma products. Doxycycline chlorohydrate ($\text{C}_{22}\text{H}_{24}\text{N}_2\text{O}_8 \bullet \text{HCl}$, $M_w = 480.90 \text{ kg mol}^{-1}$) was from Alfa Aesar. Halloysite characterization was reported in our recent publication [19].

3.2. HNTs Loading with Doxycycline Chlorohydrate

The drug loading into HNTs cavity was carried out by using a procedure well established in literature [54]. Briefly, 0.5 g of doxycycline chlorohydrate was mixed with 2 g of HNTs in 20 cm^3 of water. The dispersion was kept under vacuum for 30 min. This procedure was repeated three times before centrifugation at 8000 rpm for 20 min to separate the loaded HNTs from the supernatant. The loaded HNTs were rinsed with water and the drug loading of 4.2 wt % was determined by thermogravimetry. The experimental thermogravimetric curves are provided in Supplementary Material. The method used for drug loading calculation was detailed elsewhere [57].

3.3. Preparation of Gel Beds

The chitosan based gel beads were prepared by using the dropping technique [58]. Chitosan (2 wt %) was dissolved in water containing 0.5 wt % of acetic acid. A peristaltic pump was used to drop the chitosan solution into an aqueous solution of NaOH 1.5 M. The needle diameter was 0.4 mm and the distance from the needle to the liquid surface was 2 cm. The obtained gel beads stood in the NaOH solution overnight, and afterwards they were rinsed with water three times. The preparation

of the hybrid HNTs/Chitosan gel beads was carried out by using the same methodology. In this case, HNTs loaded with doxycycline chlorohydrate were dispersed into the chitosan solution with a polymer: HNTs weight ratio of 1:1. Some of the beads were in contact with a sodium alginate solution (2 wt %) for 10 mins and then with CaCl_2 0.1 M to cross-link the alginate polymer. Beads were dried out at 40 °C overnight.

3.4. Doxycycline Chlorohydrate Release Experiments

The release profiles in water were determined by measuring UV-VIS spectra in a quartz cuvettes without stirring. In particular, one dried bead or the equivalent amount of loaded HNTs was weighted and directly placed into a cuvette. An amount of 2 cm³ of distilled water was added and the spectra was recorded for 200 min.

3.5. Synthesis of DTAF Labeled Sodium Alginate

Alginate fluorescent labelling was carried out following the literature [59]. Sodium alginate (10 mg cm⁻³) was solubilized in sodium bicarbonate (50 mM) and 1.0 M NaOH was used to adjust the pH to 9. DTAF (concentration of 10 mg mL⁻¹ in dimethyl sulfoxide) was added at room temperature with an alginate: DTAF solutions volume ratio of 1:0.4. After one night of stirring, the mixture was dialysed in a 10 kDa cut-off dialysis tubing against phosphate-buffered saline (PBS) until the DTAF was not detected in the dialysate by UV at 490 nm.

3.6. Experimental Methods

UV-VIS spectra of doxycycline chlorohydrate were recorded by a Specord S600 (Analytik, Jena, Germany). Doxycycline chlorohydrate in water had a peak at 362 nm with an extinction coefficient of $23.6 \pm 0.3 \text{ cm}^3 \text{ mg}^{-1}$. SEM images were obtained by using a microscope ESEM FEI QUANTA 200F (FEI, Hillsboro, OR, USA) in high vacuum mode ($<6 \times 10^{-4}$ Pa). Before each SEM experiment, the surface of the sample was coated with gold in argon by means of an Edwards Sputter Coater S150A (Edwards Lifesciences, Milan, Italy) to avoid charging under an electron beam. Laser scanning confocal microscopy images were obtained using a LSM 780 instrument (Carl Zeiss, Jena, Germany) equipped with apochromatic 20× and 40× objectives and argon laser (488 nm). Images were processed using ZEN Black software (Carl Zeiss MicroImaging GmbH, Göttingen, Germany). Thermogravimetry (TG) measurements were performed by means of a Q5000 IR apparatus (TA Instruments, Milan, Italy) under nitrogen flows of 25 and 10 cm³ min⁻¹ for the sample and the balance, respectively. The sample (approximately 3 mg) was heated from room temperature to 700 °C at 10 °C min⁻¹. Calibration was carried out by following the procedure reported in literature [60].

4. Conclusions

In summary, we prepared hybrid gel beads with a chitosan rich core and an alginate rich shell containing halloysite nanotubes. The clay nanoparticles were loaded with a model drug and showed a good dispersion within the beads. The kinetics of the drug release was controlled by a core/shell structure. This work opens new perspectives into the preparation of hybrid biopolymer/nanoclay structures for drug delivery applications, and proposes a new strategy for obtaining tuned drug release.

Supplementary Materials: The following are available online at <http://www.mdpi.com/2079-6412/9/2/70/s1>, Figure S1: Thermogravimetric curves for HNTs loaded with Doxycycline chlorohydrate and their pure components (HNTs and Doxycycline chlorohydrate).

Author Contributions: Conceptualization, G.L. and R.F.; Methodology, G.C.; Validation, G.C., G.L. and R.F.; Formal Analysis, G.L.; Investigation, L.L. and F.P.; Data Curation, L.L.; Writing-Original Draft Preparation, L.L.; Writing-Review & Editing, G.L.; Supervision, G.L.; Project Administration, S.M.; Funding Acquisition, S.M. and R.F.

Acknowledgments: The work was financially supported by Progetto di ricerca e sviluppo "AGM for CuHe" (No. ARS01_00697) and the CORI 2018 project by the University of Palermo. The work was performed according

to the Russian Government Program of Competitive Growth of the Kazan Federal University. This work was funded by the subsidy allocated to the Kazan Federal University for the state assignment in the sphere of scientific activities (No. 16.2822.2017/4.6) and by RFBR (No. 18-29-11031).

Conflicts of Interest: The authors declare no conflict of interest.

References

1. Ahmed, E.M. Hydrogel: Preparation, characterization, and applications: A review. *J. Adv. Res.* **2015**, *6*, 105–121. [[CrossRef](#)]
2. Akhtar, M.F.; Hanif, M.; Ranjha, N.M. Methods of synthesis of hydrogels: A review. *Saudi Pharm. J.* **2016**, *24*, 554–559. [[CrossRef](#)] [[PubMed](#)]
3. Ullah, F.; Othman, M.B.H.; Javed, F.; Ahmad, Z.; Akil, H.M. Classification, processing and application of hydrogels: A review. *Mater. Sci. Eng. C* **2015**, *57*, 414–433. [[CrossRef](#)] [[PubMed](#)]
4. Li, Y.; Huang, G.; Zhang, X.; Li, B.; Chen, Y.; Lu, T.; Lu, T.J.; Xu, F. Magnetic Hydrogels and Their Potential Biomedical Applications. *Adv. Funct. Mater.* **2012**, *23*, 660–672. [[CrossRef](#)]
5. Cao, J.; Tan, Y.; Che, Y.; Xin, H. Novel complex gel beads composed of hydrolyzed polyacrylamide and chitosan: An effective adsorbent for the removal of heavy metal from aqueous solution. *Bioresour. Technol.* **2010**, *101*, 2558–2561. [[CrossRef](#)] [[PubMed](#)]
6. Zheng, Y.; Wang, A. Enhanced Adsorption of Ammonium Using Hydrogel Composites Based on Chitosan and Halloysite. *J. Macromol. Sci. Part A* **2009**, *47*, 33–38. [[CrossRef](#)]
7. Li, J.; Li, X.; Zhou, Z.; Ni, X.; Leong, K.W. Formation of Supramolecular Hydrogels Induced by Inclusion Complexation between Pluronics and α -Cyclodextrin. *Macromolecules* **2001**, *34*, 7236–7237. [[CrossRef](#)]
8. Dadsetan, M.; Taylor, K.E.; Yong, C.; Bajzer, Z.; Lu, L.; Yaszemski, M.J. Controlled release of doxorubicin from pH-responsive microgels. *Acta Biomater.* **2013**, *9*, 5438–5446. [[CrossRef](#)]
9. Varaprasad, K.; Raghavendra, G.M.; Jayaramudu, T.; Yallapu, M.M.; Sadiku, R. A mini review on hydrogels classification and recent developments in miscellaneous applications. *Mater. Sci. Eng. C* **2017**, *79*, 958–971. [[CrossRef](#)]
10. Ganguly, K.; Chaturvedi, K.; More, U.A.; Nadagouda, M.N.; Aminabhavi, T.M. Polysaccharide-based micro/nanohydrogels for delivering macromolecular therapeutics. *Drug Deliv. Res. Asia Pac. Reg.* **2014**, *193*, 162–173. [[CrossRef](#)]
11. Wei, Z.; Yang, J.H.; Liu, Z.Q.; Xu, F.; Zhou, J.X.; Zrínyi, M.; Osada, Y.; Chen, Y.M. Novel biocompatible polysaccharide-based self-healing hydrogel. *Adv. Funct. Mater.* **2015**, *25*, 1352–1359. [[CrossRef](#)]
12. Sahiner, N.; Godbey, W.T.; McPherson, G.L.; John, V.T. Microgel, nanogel and hydrogel–hydrogel semi-IPN composites for biomedical applications: Synthesis and characterization. *Colloid Polym. Sci.* **2006**, *284*, 1121–1129. [[CrossRef](#)]
13. Liu, K.-H.; Liu, T.-Y.; Chen, S.-Y.; Liu, D.-M. Drug release behavior of chitosan–montmorillonite nanocomposite hydrogels following electrostimulation. *Acta Biomater.* **2008**, *4*, 1038–1045. [[CrossRef](#)]
14. Yang, H.; Hua, S.; Wang, W.; Wang, A. Composite Hydrogel Beads Based on Chitosan and Laponite: Preparation, Swelling, and Drug Release Behaviour. *Iran. Polym. J.* **2011**, *20*, 479–490.
15. Bonifacio, M.A.; Gentile, P.; Ferreira, A.M.; Cometa, S.; De Giglio, E. Insight into halloysite nanotubes-loaded gellan gum hydrogels for soft tissue engineering applications. *Carbohydr. Polym.* **2017**, *163*, 280–291. [[CrossRef](#)] [[PubMed](#)]
16. Lee, H.; Ryu, J.; Kim, D.; Joo, Y.; Lee, S.U.; Sohn, D. Preparation of an imogolite/poly(acrylic acid) hybrid gel. *J. Colloid Interface Sci.* **2013**, *406*, 165–171. [[CrossRef](#)] [[PubMed](#)]
17. Lazzara, G.; Cavallaro, G.; Panchal, A.; Fakhrullin, R.; Stavitskaya, A.; Vinokurov, V.; Lvov, Y. An assembly of organic-inorganic composites using halloysite clay nanotubes. *Curr. Opin. Colloid Interface Sci.* **2018**, *35*, 42–50. [[CrossRef](#)]
18. Lisuzzo, L.; Cavallaro, G.; Parisi, F.; Milioto, S.; Lazzara, G. Colloidal stability of halloysite clay nanotubes. *Ceram. Int.* **2018**. [[CrossRef](#)]
19. Cavallaro, G.; Chiappisi, L.; Pasbakhsh, P.; Gradzielski, M.; Lazzara, G. A structural comparison of halloysite nanotubes of different origin by Small-Angle Neutron Scattering (SANS) and Electric Birefringence. *Appl. Clay Sci.* **2018**, *160*, 71–80. [[CrossRef](#)]

20. Lvov, Y.M.; Shchukin, D.G.; Mohwald, H.; Price, R.R. Halloysite Clay Nanotubes for Controlled Release of Protective Agents. *ACS Nano* **2008**, *2*, 814–820. [[CrossRef](#)]
21. Luo, Z.; Song, H.; Feng, X.; Run, M.; Cui, H.; Wu, L.; Gao, J.; Wang, Z. Liquid Crystalline Phase Behavior and Sol–Gel Transition in Aqueous Halloysite Nanotube Dispersions. *Langmuir* **2013**, *29*, 12358–12366. [[CrossRef](#)] [[PubMed](#)]
22. Viseras, C.; Cerezo, P.; Sanchez, R.; Salcedo, I.; Aguzzi, C. Current challenges in clay minerals for drug delivery. *Appl. Clay Sci.* **2010**, *48*, 291–295. [[CrossRef](#)]
23. Joussein, E.; Petit, S.; Churchman, G.J.; Theng, B.; Righi, D.; Delvaux, B. Halloysite clay minerals—A review. *Clay Miner.* **2005**, *40*, 383–426. [[CrossRef](#)]
24. Pasbakhsh, P.; Churchman, G.J.; Keeling, J.L. Characterisation of properties of various halloysites relevant to their use as nanotubes and microfibre fillers. *Appl. Clay Sci.* **2013**, *74*, 47–57. [[CrossRef](#)]
25. Cavallaro, G.; Lazzara, G.; Milioto, S. Exploiting the Colloidal Stability and Solubilization Ability of Clay Nanotubes/Ionic Surfactant Hybrid Nanomaterials. *J. Phys. Chem. C* **2012**, *116*, 21932–21938. [[CrossRef](#)]
26. Bertolino, V.; Cavallaro, G.; Lazzara, G.; Milioto, S.; Parisi, F. Biopolymer-Targeted Adsorption onto Halloysite Nanotubes in Aqueous Media. *Langmuir* **2017**, *33*, 3317–3323. [[CrossRef](#)]
27. Abdullayev, E.; Price, R.; Shchukin, D.; Lvov, Y. Halloysite Tubes as Nanocontainers for Anticorrosion Coating with Benzotriazole. *ACS Appl. Mater. Interfaces* **2009**, *1*, 1437–1443. [[CrossRef](#)]
28. Cavallaro, G.; Lazzara, G.; Milioto, S.; Palmisano, G.; Parisi, F. Halloysite nanotube with fluorinated lumen: Non-foaming nanocontainer for storage and controlled release of oxygen in aqueous media. *J. Colloid Interface Sci.* **2014**, *417*, 66–71. [[CrossRef](#)]
29. Aguzzi, C.; Viseras, C.; Cerezo, P.; Salcedo, I.; Sánchez-Espejo, R.; Valenzuela, C. Release kinetics of 5-aminosalicylic acid from halloysite. *Colloids Surf. B Biointerfaces* **2013**, *105*, 75–80. [[CrossRef](#)]
30. Fakhrullina, G.I.; Akhatova, F.S.; Lvov, Y.M.; Fakhrullin, R.F. Toxicity of halloysite clay nanotubes in vivo: A *Caenorhabditis elegans* study. *Environ. Sci. Nano* **2015**, *2*, 54–59. [[CrossRef](#)]
31. Zhao, Y.; Abdullayev, E.; Vasiliev, A.; Lvov, Y. Halloysite nanotubule clay for efficient water purification. *J. Colloid Interface Sci.* **2013**, *406*, 121–129. [[CrossRef](#)] [[PubMed](#)]
32. Cavallaro, G.; Lazzara, G.; Milioto, S.; Parisi, F.; Sanzillo, V. Modified Halloysite Nanotubes: Nanoarchitectures for Enhancing the Capture of Oils from Vapor and Liquid Phases. *ACS Appl. Mater. Interfaces* **2014**, *6*, 606–612. [[CrossRef](#)]
33. Luo, P.; Zhang, J.; Zhang, B.; Wang, J.; Zhao, Y.; Liu, J. Preparation and Characterization of Silane Coupling Agent Modified Halloysite for Cr(VI) Removal. *Ind. Eng. Chem. Res.* **2011**, *50*, 10246–10252. [[CrossRef](#)]
34. Zhao, M.; Liu, P. Adsorption behavior of methylene blue on halloysite nanotubes. *Microporous Mesoporous Mater.* **2008**, *112*, 419–424. [[CrossRef](#)]
35. Hermawan, A.A.; Chang, J.W.; Pasbakhsh, P.; Hart, F.; Talei, A. Halloysite nanotubes as a fine grained material for heavy metal ions removal in tropical biofiltration systems. *Appl. Clay Sci.* **2018**, *160*, 106–115. [[CrossRef](#)]
36. Cavallaro, G.; Milioto, S.; Parisi, F.; Lazzara, G. Halloysite Nanotubes Loaded with Calcium Hydroxide: Alkaline Fillers for the Deacidification of Waterlogged Archeological Woods. *ACS Appl. Mater. Interfaces* **2018**, *10*, 27355–27364. [[CrossRef](#)] [[PubMed](#)]
37. Cavallaro, G.; Lazzara, G.; Milioto, S.; Parisi, F. Halloysite Nanotubes for Cleaning, Consolidation and Protection. *Chem. Rec.* **2018**, *18*, 940–949. [[CrossRef](#)]
38. Lvov, Y.; Abdullayev, E. Functional polymer–clay nanotube composites with sustained release of chemical agents. *Prog. Polym. Sci.* **2013**, *38*, 1690–1719. [[CrossRef](#)]
39. Abdullayev, E.; Sakakibara, K.; Okamoto, K.; Wei, W.; Ariga, K.; Lvov, Y. Natural Tubule Clay Template Synthesis of Silver Nanorods for Antibacterial Composite Coating. *ACS Appl. Mater. Interfaces* **2011**, *3*, 4040–4046. [[CrossRef](#)]
40. Liu, M.; Wu, C.; Jiao, Y.; Xiong, S.; Zhou, C. Chitosan-halloysite nanotubes nanocomposite scaffolds for tissue engineering. *J. Mater. Chem. B* **2013**, *1*, 2078–2089. [[CrossRef](#)]
41. Zhang, H.; Cheng, C.; Song, H.; Bai, L.; Cheng, Y.; Ba, X.; Wu, Y. A facile one-step grafting of polyphosphonium onto halloysite nanotubes initiated by Ce(IV). *Chem. Commun.* **2019**. [[CrossRef](#)] [[PubMed](#)]
42. Liu, F.; Bai, L.; Zhang, H.; Song, H.; Hu, L.; Wu, Y.; Ba, X. Smart H₂O₂-Responsive Drug Delivery System Made by Halloysite Nanotubes and Carbohydrate Polymers. *ACS Appl. Mater. Interfaces* **2017**, *9*, 31626–31633. [[CrossRef](#)] [[PubMed](#)]

43. Wei, W.; Minullina, R.; Abdullayev, E.; Fakhrullin, R.; Mills, D.; Lvov, Y. Enhanced efficiency of antiseptics with sustained release from clay nanotubes. *RSC Adv.* **2014**, *4*, 488–494. [[CrossRef](#)]
44. Kurczewska, J.; Ceglowski, M.; Messyasz, B.; Schroeder, G. Dendrimer-functionalized halloysite nanotubes for effective drug delivery. *Appl. Clay Sci.* **2018**, *153*, 134–143. [[CrossRef](#)]
45. Gorrasi, G.; Pantani, R.; Murariu, M.; Dubois, P. PLA/Halloysite Nanocomposite Films: Water Vapor Barrier Properties and Specific Key Characteristics. *Macromol. Mater. Eng.* **2014**, *299*, 104–115. [[CrossRef](#)]
46. De Silva, R.T.; Pasbakhsh, P.; Goh, K.L.; Chai, S.-P.; Ismail, H. Physico-chemical characterisation of chitosan/halloysite composite membranes. *Polym. Test.* **2013**, *32*, 265–271. [[CrossRef](#)]
47. He, Y.; Kong, W.; Wang, W.; Liu, T.; Liu, Y.; Gong, Q.; Gao, J. Modified natural halloysite/potato starch composite films. *Carbohydr. Polym.* **2012**, *87*, 2706–2711. [[CrossRef](#)]
48. Biddeci, G.; Cavallaro, G.; Di Blasi, F.; Lazzara, G.; Massaro, M.; Milioto, S.; Parisi, F.; Riela, S.; Spinelli, G. Halloysite nanotubes loaded with peppermint essential oil as filler for functional biopolymer film. *Carbohydr. Polym.* **2016**, *152*, 548–557. [[CrossRef](#)]
49. Sun, P.; Liu, G.; Lv, D.; Dong, X.; Wu, J.; Wang, D. Simultaneous improvement in strength, toughness, and thermal stability of epoxy/halloysite nanotubes composites by interfacial modification. *J. Appl. Polym. Sci.* **2016**, *133*. [[CrossRef](#)]
50. Kim, M.; Kim, S.; Kim, T.; Lee, D.K.; Seo, B.; Lim, C.-S. Mechanical and Thermal Properties of Epoxy Composites Containing Zirconium Oxide Impregnated Halloysite Nanotubes. *Coatings* **2017**, *7*, 231. [[CrossRef](#)]
51. Cavallaro, G.; Lazzara, G.; Lisuzzo, L.; Milioto, S.; Parisi, F. Selective adsorption of oppositely charged PNIPAAm on halloysite surfaces: A route to thermo-responsive nanocarriers. *Nanotechnology* **2018**, *29*, 325702. [[CrossRef](#)]
52. Cavallaro, G.; Danilushkina, A.A.; Evtugyn, V.G.; Lazzara, G.; Milioto, S.; Parisi, F.; Rozhina, E.V.; Fakhrullin, R.F. Halloysite Nanotubes: Controlled Access and Release by Smart Gates. *Nanomaterials* **2017**, *7*, 199. [[CrossRef](#)] [[PubMed](#)]
53. Cavallaro, G.; Lazzara, G.; Milioto, S.; Parisi, F.; Evtugyn, V.; Rozhina, E.; Fakhrullin, R. Nanohydrogel Formation within the Halloysite Lumen for Triggered and Sustained Release. *ACS Appl. Mater. Interfaces* **2018**, *10*, 8265–8273. [[CrossRef](#)] [[PubMed](#)]
54. Lvov, Y.M.; DeVilliers, M.M.; Fakhrullin, R.F. The application of halloysite tubule nanoclay in drug delivery. *Expert Opin. Drug Deliv.* **2016**, *13*, 977–986. [[CrossRef](#)]
55. Cavallaro, G.; Gianguzza, A.; Lazzara, G.; Milioto, S.; Piazzese, D. Alginate gel beads filled with halloysite nanotubes. *Appl. Clay Sci.* **2013**, *72*, 132–137. [[CrossRef](#)]
56. Lisuzzo, L.; Cavallaro, G.; Lazzara, G.; Milioto, S.; Parisi, F.; Stetsyshyn, Y. Stability of Halloysite, Imogolite, and Boron Nitride Nanotubes in Solvent Media. *Appl. Sci.* **2018**, *8*, 1068. [[CrossRef](#)]
57. Cavallaro, G.; Lazzara, G.; Milioto, S.; Parisi, F.; Ruisi, F. Nanocomposites based on esterified colophony and halloysite clay nanotubes as consolidants for waterlogged archaeological woods. *Cellulose* **2017**, *24*, 3367–3376. [[CrossRef](#)]
58. Kofuji, K.; Shibata, K.; Murata, Y.; Miyamoto, E.; Kawashima, S. Preparation and Drug Retention of Biodegradable Chitosan Gel Beads. *Chem. Pharm. Bull. (Tokyo)* **1999**, *47*, 1494–1496. [[CrossRef](#)]
59. Mackie, A.; Bajka, B.; Rigby, N. Roles for dietary fibre in the upper GI tract: The importance of viscosity. *Food Res. Int.* **2016**, *88*, 234–238. [[CrossRef](#)]
60. Blanco, I.; Abate, L.; Bottino, F.A.; Bottino, P. Thermal degradation of hepta cyclopentyl, mono phenyl-polyhedral oligomeric silsesquioxane (hcp-POSS)/polystyrene (PS) nanocomposites. *Polym. Degrad. Stabil.* **2012**, *97*, 849–855. [[CrossRef](#)]

